Journal of Hydrology 638 (2024) 131483

Contents lists available at ScienceDirect

Journal of Hydrology

journal homepage: www.elsevier.com/locate/jhydrol

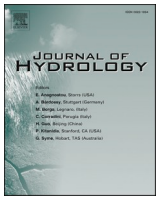

Research papers

Calibrating the lyne-hollick filter for baseflow separation based on catchment response time

Eszter D. Nagy [a,*], Jozsef Szilagyi [a,b], Peter Torma [a,c]

[a] National Laboratory for Water Science and Water Security, Budapest University of Technology and Economics, Faculty of Civil Engineering, Department of Hydraulic and Water Resources Engineering, Budapest, Hungary
[b] Conservation and Survey Division, School of Natural Resources, University of Nebraska-Lincoln, Lincoln, Nebraska, USA
[c] HUN-REN–SZTE Research Group for Photoacoustic Monitoring of Environmental Processes, Szeged, Hungary

ARTICLE INFO

This manuscript was handled by C. Corradini, Editor-in-Chief, with the assistance of Corrado Corradini, Associate Editor?.

Keywords:
Lyne-Hollick filter
Digital recursive filter
Baseflow separation
Catchment response time
Time to equilibrium
Time of concentration
Lag time
Kinematic wave theory

ABSTRACT

The physically meaningful separation of baseflow from the observed streamflow time series is still an unresolved problem in hydrology. This study provides a novel method that builds upon catchment response time to formulate an optimization criterion for calibrating the Lyne-Hollick filter. Catchment response time parameters, including time of concentration (T_c) and time to equilibrium (T_e), can be derived from observed precipitation and discharge time series. A range for the ratio of these two has already been derived on a physical basis. In the presented approach, the parameter of the Lyne-Hollick filter is calibrated so that the ratio of T_c and T_e falls between a physically plausible range. The proposed method was tested in 25 catchments, and the results were compared to those derived in a previous study. The Pearson correlation coefficient improved from 0.654 to 0.862 between T_c and the lag time when applying the proposed calibration procedure.

1. Introduction

The separation of baseflow, as the contribution of groundwater to total stream flow, is a common practice in hydrology. The quantification of baseflow and direct runoff has many uses. By knowing the event-specific surface runoff (i.e., quick-storm response) time series, flood analysis, the derivation of the unit hydrograph, and the calibration of rainfall-runoff as well as runoff-routing models, just to name a few direct applications, can all be carried out (Nathan and McMahon, 1990). Baseflow might be used to derive low flow statistics, which can be useful in many fields of water management, such as water supply, hydro-ecology, water quality management, and aquifer characterization (Szilagyi, 2004). As Nathan and McMahon (1990) quote, baseflow separation is "one of the most desperate analysis techniques in use in hydrology". Indeed, up to date, there is no generally accepted methodology to separate direct/surface runoff and baseflow from streamflow time series.

The existence of numerous methods muddles the choice of the most appropriate method. As an illustration, Nejadhashemi et al. (2009) collected 40 baseflow separation methods, while Mei and Anagnostou (2015) also provided a nice collection of recent approaches. Furey and Gupta (2001) sorted the efforts to separate baseflow from streamflow into four groups, namely, (1) geochemical, (2) graphical, (3) analytical, and (4) filtering. Geochemical measurements can be made by the use of isotopes (Stadnyk et al., 2015), sediment load (Zheng, 2015), or electrical conductivity (Lott and Stewart, 2013; Stewart et al., 2007), but such measurements are sparse compared to the availability of continuous streamflow data. Graphical methods are the most exposed to subjectivity through user-made, often arbitrary, assumptions. Analytical approaches are based on fundamental theories of groundwater and surface flow (Nejadhashemi et al., 2009). Despite having a physical basis, these latter methods are often complex and accurate only if proper input parameter values are given (Nejadhashemi et al., 2009). For example, the method proposed by Meshgi et al., (2014,2015) utilizes groundwater table fluctuations to estimate baseflow time series empirically, hence requires groundwater observations. Digital filters can be further sorted based on the number of parameters involved (one, two, or multiple). One of the most often used one-parameter methods is the

* Corresponding author at: 1111 Budapest, Muegyetem rakpart 3., Hungary.
E-mail address: nagy.eszter@emk.bme.hu (E.D. Nagy).

https://doi.org/10.1016/j.jhydrol.2024.131483
Received 27 September 2023; Received in revised form 20 February 2024; Accepted 22 May 2024
Available online 13 June 2024

Lyne-Hollick (LH) filter (Lyne and Hollick, 1979; Nathan and McMahon, 1990).

Like every baseflow separation method, the LH filter also has its merits and drawbacks. This recursive digital filter was originally used for signal analysis and processing (Nathan and McMahon, 1990). The analogy of filtering high-frequency signals such as quick-storm response, led to the application of the LH filter for baseflow separation. However, the approach lacks any physical basis, as emphasized by many authors (Duncan, 2019; Furey and Gupta, 2001; Giani et al., 2021; Nathan and McMahon, 1990; Schwartz, 2007; Xie et al., 2020). Additionally, applications show varying performance for this filter. While the LH filter performed better over a more extensive range of conditions than the other two filters (Boughton, 1988; Eckhardt, 2005) tested by Li et al. (2014), it ranked last in the study of Xie et al. (2020). The two main aspects of the LH filter's application are the i) number of passes required, and; ii) selection of its single parameter value. The parameter affects the degree of baseflow attenuation, and the number of passes determines the degree of smoothing (Nathan and McMahon, 1990). The filter was initially applied three times (forward, backward, and forward again) by Nathan and McMahon (1990). The reverse pass aims to nullify any phase distortion. Different authors applied different number of passes since then. Ladson et al. (2013) report that the optimal number of passes depends on the time step of the streamflow time series, while Graszkiewicz et al. (2011) suggest nine passes for hourly time series. However, such a high number of passes are not reported elsewhere. The smoothing effect, and thus the reduction of baseflow caused by the additional passes, is clear. For example, Arnold et al. (1995) reported a 17 % and 10 % decrease in baseflow due to the second and third pass. On the other hand, Zhang et al. (2017) state that using multiple passes can only slightly improve or deteriorate baseflow index estimates. Besides the number of passes, estimating the filter parameter value is an even more significant application issue.

The selection of an appropriate parameter value is an open question (Landson, 2013). Nathan and McMahon (1990) found a single parameter value (0.925) applicable to their study catchments using daily streamflow data. Many authors adopted this value since then (e.g., Jolánkai and Koncsos, 2018; Xie et al., 2020; Zheng, 2015), but other studies report a vastly expansive range of values. Even though many studies compared the performance of recursive digital filters (Nejadhashemi et al., 2009; Chapman, 1999; Eckhardt, 2005, 2008; Partington et al., 2012), only a very few attempted to calibrate the parameter of the LH filter using commonly available data, such as the discharge and precipitation time series. Unfortunately, standard calibration procedures often applied in hydrological modelling (Babovic and Wu, 1994; Madsen et al., 2002) cannot be used in the case of the LH filter since, typically, no observations are available for baseflow. Szilagyi (2004) optimized the parameter value relying on an empirical relationship (Linsley et al., 1958), relating catchment area and the watershed-specific time delay (i.e., the mean elapsed time between the peak of streamflow and the first instant when streamflow becomes dominated by baseflow). This relationship is, however, not necessarily valid for all catchments (Stewart et al., 2007). Nejadhashemi et al. (2007) calibrated the LH filter using the output of another separation method (Boughton, 1988), which still requires user-defined runoff cessation points on the hydrograph. Some authors suggest visual fitting of the separated baseflow curve (Giani et al., 2021; Grimaldi et al., 2012; Nagy et al., 2021; Tang and Carey, 2017), but this approach is undoubtedly the most subjective. Here, we propose a new procedure that builds on catchment response time parameters.

Even though some of the catchment response time parameters date back more than a 150 years (Beven, 2020), they are still intensively researched (Almeida et al., 2022), and several issues remain around them. The most often used response time parameters include time of concentration (T_c), time to equilibrium (T_e), lag time (T_L), and time to peak (Langridge et al., 2020). Following the reasoning of Giani et al. (2021), the authors prefer to use catchment response time as a general term and only discuss specific parameters when it is relevant. The possibilities to estimate response time parameters are also manifold. The main approaches include procedures based on i) empirical or semi-empirical formulas; ii) measured data, and; iii) hydraulic equations. Indirect estimation of response time parameters is possible by using registered rainfall and runoff time series. However, this method includes the application of graphical definitions, i.e., defining the response time parameters as a time difference between two points of the hyeto- and hydrographs. Conclusively, the identification of rainfall-runoff events and the separation of baseflow and direct runoff is required. Equations derived on a hydraulic basis often have several parameters which are difficult to obtain. However, the relationship between T_c and T_e can be derived on a hydraulic basis.

The physically based relationship and the graphical definitions of T_e and T_c can be used to formulate an optimization criterion for baseflow separation using the LH filter. Beven (2020) thoroughly discussed the difference between these two response time parameters. From the hydraulic point of view, T_c can be calculated by integrating flow velocity along the longest flow path, while T_e needs to be calculated using wave celerity instead of flow velocity. The kinematic wave theory provides a suitable framework to calculate the velocity- and celerity-based response times. Wong (2003) derived values for the T_c/T_e ratios for both plane and channel flow, including various hydraulic conditions. Assuming that the ratio of the two parameters when derived utilizing the graphical definitions should yield values in the same range as when derived from the kinematic wave theory, baseflow separation can be optimized since it strongly influences the end of direct runoff, hence the value of T_c.

The proposed calibration method was tested for a set of study catchments. The results are compared to a previously performed manual calibration, and a sensitivity analysis is also included. The results are compared to other values derived in the literature. A downloadable script is also provided, including sample data and its application.

2. Study area

The study area consists of 25 medium-sized western Hungarian catchments, as depicted in Fig. 1. The catchments' main properties are presented in Table 1. The catchment area ranges from 20.2 km^2 to 810 km^2, with a median of 269 km^2. The land use proportions vary between the catchments. The ratio of urban areas is between 0.28 % and 5.87 %, while forested areas cover 3.8–64 % of the catchments. The maximum elevation difference covers two orders of magnitude between 90 m and 1394 m. Mean annual runoff and precipitation are in the range of 20.4–197.3 mm and 669–832 mm, respectively. This set of catchments is a subset of the ones studied in previous works by Nagy et al., (2021,2022), where further description of the study area is presented.

The time series employed consist of hourly precipitation and discharge data recorded between 2001 and 2017. Discharge was derived from the registered water levels using a rating curve provided by the local water directorates, while precipitation was downloaded from the ECMWF Era5-Land database (Copernicus Climate Change Service, 2019). This reanalysis dataset contains hourly precipitation time series at a spatial resolution of 0.1° x 0.1° (~9 km x ~ 9 km) dating back to 1950. Reanalysis data is a combination of observations and modeled data, therefore, it might be biased due to the spatial interpolation and the relatively coarse spatial resolution. Since precipitation gauging station data was not available for every catchment, reanalysis data was used uniformly for each catchment.

3. Methodology

The workflow of the proposed calibration routine is summarized in Fig. 2. The calculation steps, variable names, and other specifications (e.g., required inputs) are explained in details below. The algorithm has been implemented in MATLAB and RStudio, and is freely available from

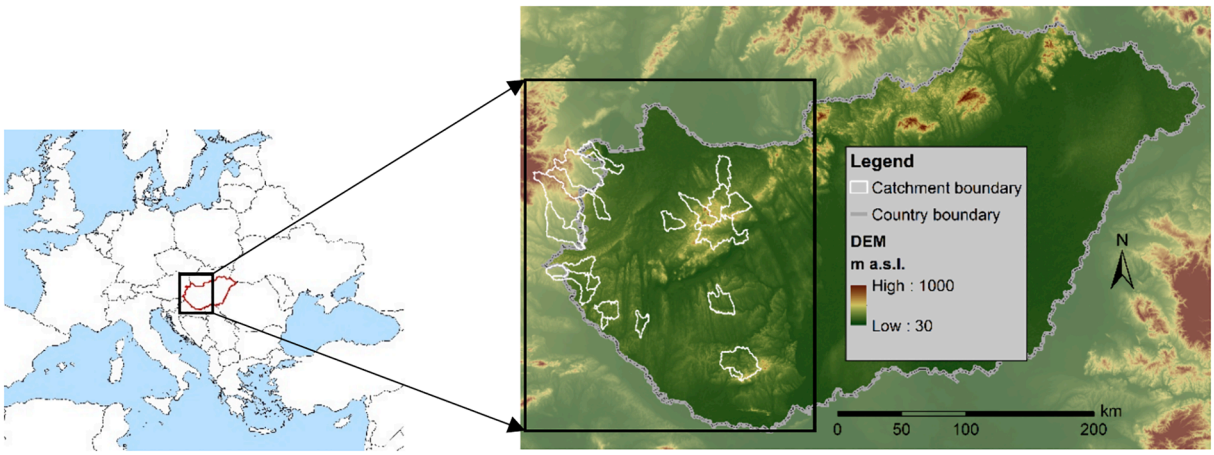

Fig. 1. Overview of the study catchments.

Table 1
Properties of the study catchments: catchment area (A), the portion of catchment covered with urban areas (A_u) and forested areas (A_f), length of the longest flow path (L), maximum elevation difference (H), mean annual runoff (MAR) and mean annual precipitation (MAP).

ID	A [km^2]	A_u [%]	A_f [%]	L [km]	H [m]	MAR [mm]	MAP [mm]	ID	A [km^2]	A_u [%]	A_f [%]	L [km]	H [m]	MAR [mm]	MAP [mm]
1	181	2.88	49.0	32.8	180	110	774	14	455	1.26	24.5	56.5	232	90.2	785
2	137	6.28	40.2	30.6	407	57.6	750	15	98.8	4.97	31.0	23.3	164	92.6	752
3	471	3.32	48.1	41.8	484	97.9	749	16	133	8.57	7.48	31.8	157	56.9	712
4	33.8	1.89	64.0	12.2	170	57.2	775	17	77.5	1.91	61.2	17.3	89.9	51.7	777
5	46.1	1.28	55.6	15.2	402	85.5	758	18	269	2.92	23.0	31.0	189	59.9	669
6	284	3.99	43.9	42.8	492	59.7	727	19	667	5.99	45.5	66.7	1394	128	832
7	487	2.05	3.83	70.2	540	55.3	687	20	810	0.53	5.37	95.1	218	61.3	832
8	242	3.86	29.2	33.3	411	84.7	710	21	435	4.79	46.3	66.1	281	197	768
9	269	3.67	51.7	54.1	578	43.2	750	22	592	4.93	46.6	69.6	674	135	803
10	290	3.74	59.7	54.3	638	20.4	818	23	20.2	1.39	45.4	8.94	186	118	748
11	149	3.15	22.7	31.3	299	53.2	711	24	508	7.30	31.8	65.2	532	62.5	715
12	353	4.46	7.99	57.4	437	78.9	723	25	188	3.16	53.9	30.1	144	81.1	765
13	113	0.28	42.5	21.9	192	132	759								

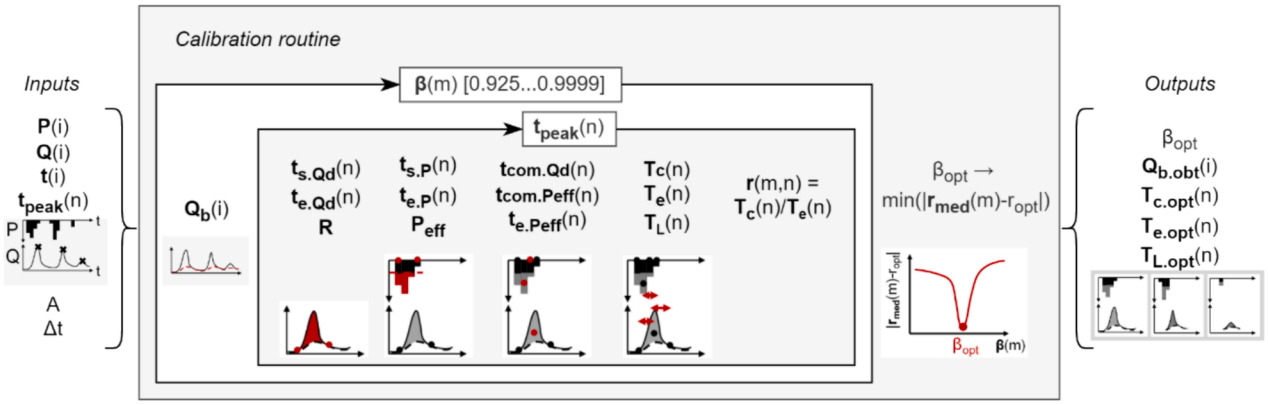

Fig. 2. Workflow for the Lyne-Hollick filter parameter calibration.

here: https://github.com/EszterDNagy/baseflow_calibration.

The required inputs for the LH filter calibration are the following: precipitation time series (P [mm]), discharge time series (Q [m^3/s]), related date time array (t), time instants of user-specified flood peaks (t_{peak}), catchment area (A [km^2]), the time step of the time series (Δt [s]), and a variable denoting whether the results should be plotted. The required format of these variables is described in the script descriptions. The time series must have the same length and uniform time step. In addition, the user needs to specify an arbitrary number of flood-peak time occurrences. These events will be used for calibration. The algorithm works best for regular single-peaked flood events (see further reasoning below). The user might consider the following during flood peak selection: i) selecting single-peak events only; ii) checking the presence of recorded rainfall data sufficient enough to produce the related flood event; iii) inspecting whether the selected floods have smooth rising and falling limbs, and; iv) ensuring that the selected floods are representative for the given catchment in terms of shape and size. Catchment area and a constant time step are required to calculate runoff (R [mm]) from surface flow (Q_d [m^3/s]). Once the initial data are provided, the calibration routine performs the calibration of the LH filter

parameter.

The calibration procedure tests a range of values for the parameter of the applied separation method. The LH filter can be written as:

$$Q_d(t) = \beta \bullet Q_d(t-1) + \frac{1+\beta}{2}[Q(t) - Q(t-1)]$$

where $Q_d(t)$ [m^3/s] and $Q_d(t\text{-}1)$ [m^3/s] are the direct runoff at times t and t-1, $Q(t)$ [m^3/s] and $Q(t\text{-}1)$ [m^3/s] are the observed total runoff at times t and t-1, and β [-] is the recursive filter parameter. The baseflow is thus defined as $Q_b = Q - Q_d$. The recursive filter is applied three times (forward–backward-forward) to minimize phase distortion effects on the peak values (Nathan and McMahon, 1990). After baseflow is separated for a given value of β, the user-defined events are examined individually to define the required time instants for calculating the time parameters.

First, the start and end time of the runoff event are identified using the separated baseflow time series. The start and end points ($t_{s.Qd}$, $t_{e.Qd}$) are defined as the first and last time instants before and after the peak when baseflow reaches 90 % of the total flow. Second, direct runoff (R [mm]) for the given event can be calculated by summing direct runoff between the start and end points of the runoff event. This is where the catchment area and the defined time step are used. Effective precipitation can be later derived, assuming direct runoff equals the effective precipitation. But first, the contributing precipitation event needs to be assessed.

The precipitation event generating the given runoff event is defined between the end of direct runoff ($t_{e.Qd}$) and some time instant before the start of runoff. The end of precipitation ($t_{e.P}$) is defined as the first non-zero element of the precipitation time series before the end of direct runoff ($t_{e.Qd}$) (i.e., going backward in time starting at $t_{e.Qd}$). For the start of precipitation ($t_{s.P}$), the algorithm searches for the first null precipitation before the start of direct runoff ($t_{s.Qd}$). If the precipitation between this point and the end of precipitation is less than the total direct runoff (R) (i.e., the amount of precipitation is not sufficient to generate the observed direct runoff), the algorithm adds another 'wave' of precipitation to the previously defined one. This way, short periods of zero precipitation can be eliminated in the contributing precipitation event. The start of total precipitation is defined at the first non-zero precipitation value ($t_{s.P}$). The effective precipitation (P_{eff} [mm]) is calculated using a simple constant loss method, hence, no additional parameter needs to be introduced in the process. The loss rate is increased until the sum of effective precipitation ($\sum P_{eff}$) equals the sum of direct runoff ($\sum R$).

Further time instants required for calculating graphical definitions must be calculated. The center of mass is assessed for both direct runoff ($t_{com.Qd}$) and effective precipitation ($t_{com.Peff}$). In addition, the end of effective precipitation is also required ($t_{e.Peff}$).

The applied graphical definitions enable the calculation of the time of concentration (T_c [hr]), the time to equilibrium (T_e [hr]), and the lag time (T_L [hr]). However, the calculation of T_L is not required for the optimization of β. The applied graphical definitions are the following:

- The time of concentration is calculated as the time difference between the end of effective rainfall and the end of direct runoff ($T_c = t_{e.Qd} - t_{e.Peff}$).
- Time to equilibrium is defined as the time elapsed between the start of total rainfall and the peak of total runoff ($T_e = t_{peak} - t_{s.P}$).
- The difference between the center of mass of total precipitation and the center of mass of direct runoff yields the lag time ($T_L = t_{com.Qd} - t_{com.Peff}$).

Alternative versions of the graphical definitions for T_L and T_c can be found in the literature (Grimaldi et al., 2012). The implemented definitions are the most often used versions. However, the effect of using another definition for T_c is examined in the sensitivity analysis. Once the response time values were derived for each event and each value of β, they can be used in the calibration criteria.

The calibration criterion was formulated on a physical basis. Wong (2003) reported $r = T_c/T_e$ ratios for overland plane and channel flow derived from the kinematic wave theory. In the case of an overland plane, the ratio of these two response time parameters varies between 1.5 and 3.0 for turbulent and laminar flow conditions, respectively. Depending on the channel shape, the same ratio might fall between 1.0 and 1.667 for open channel flow. The values derived for wide rectangular and parabolic channel shapes, which are dominant in the study area, the ratios are 1.667 and 1.444, respectively. Naturally, the ratio derived from the graphical definitions might not strictly reproduce the theoretical values. The reasons for this might be i) the assumption of dry initial conditions and steady rainfall for the definition of T_e is seldom true in natural catchments (Beven, 2020); ii) the observed time series, especially precipitation, might be biased; iii) often a mixture of the above mentioned hydraulic conditions are present on a real catchment. Still, since these effects might work simultaneously and their effect on response time might cancel each other out, the T_c/T_e ratios can be expected to fall in the above-specified interval, i.e., $r \in \{1.5 \ldots 3\}$. Since the baseflow separation affects the derived direct runoff and effective precipitation, it will have an effect on the defined time instants, hence influencing the values of T_c and T_e. The calibrated, optimal value of the filter parameter β (β_{opt}) is defined by taking the median of the event-based T_c/T_e ratios (r_{med}) and searching for the smallest absolute difference compared to an optimal value of this ratio, r_{opt}. This optimal value was defined as $r_{opt} = 2.25$, being in the middle of the possible range of values. After finding the best value for β (β_{opt}), all related results can be reported.

The response time parameters ($T_{c.opt}$, $T_{e.opt}$, and $T_{L.opt}$) obtained by using the optimal parameter filter (β_{opt}), and the corresponding time series of baseflow ($Q_{b.opt}$) are the outcomes of the calibration routine. If plotting is enabled, a figure containing all rainfall-runoff events (including direct runoff and effective precipitation) is created.

The performance of the proposed calibration procedure cannot be validated through observed data since the actual value of baseflow is considered unknown (Szilagyi, 2004), and tracer measurements are not available on the study catchments. The calibrated β values are examined through the findings of previous studies. The value of the baseflow index ($BFI = \sum Q_b / \sum Q$ [-]) is also discussed. The sensitivity of the proposed method is tested in terms of the i) 90 % threshold value when defining the start and end of direct runoff; ii) T_c definition; iii) choice of $r_{opt} = 2.25$, and; iv) number of events used for calibration. Some new aspects of the LH filter in relation to the sensitivity analysis are also discovered. The sensitivity analysis was only performed for one catchment with the highest number of rainfall-runoff events.

4. Results

The above described calibration procedure was tested on 25 Hungarian catchments (see the Study Area section) having flood events between 5 and 42. The number of events, calibrated parameter values, and the corresponding baseflow indices are presented in Table 2. β_{opt} varies between 0.9950 and 0.9996, while BFI ranges from 0.334 to 0.868. Fig. 3 provides an example of the resulting figure using the MATLAB code.

The evaluation of response time parameters using several graphical definitions was performed in a previous study (Nagy et al., 2021), which included the manual calibration of the filter parameter. The resulting T_L and T_c values were compared for both the event-based and the catchment-wise median values (see Fig. 4). The linear relationship between the two response time parameters grew stronger due to the calibration procedure. The Pearson correlation coefficient increased from 0.891 to 0.968 and from 0.654 to 0.862 for the medians and the event-based values, respectively. It is also visible that T_c generally increased. This is plausible since the β_{opt} values are generally larger than the manually calibrated parameters, leading to lower baseflow and longer-

Table 2
Results of the calibration process: number of events used (n), the calibrated value of the filter parameter (β_{opt}), and the baseflow index (BFI).

ID	n [pcs]	β_{opt} [-]	BFI [-]	ID	n [pcs]	β_{opt} [-]	BFI [-]
1	13	0.998	0.47	14	14	0.9993	0.49
2	41	0.997	0.69	15	18	0.9994	0.53
3	31	0.998	0.61	16	7	0.998	0.72
4	9	0.9994	0.40	17	13	0.998	0.33
5	10	0.999	0.58	18	12	0.9993	0.63
6	16	0.9992	0.54	19	22	0.999	0.57
7	19	0.998	0.68	20	30	0.9996	0.41
8	16	0.9994	0.57	21	20	0.9995	0.52
9	9	0.998	0.63	22	30	0.998	0.73
10	16	0.997	0.73	23	10	0.998	0.77
11	5	0.997	0.67	24	28	0.996	0.87
12	42	0.995	0.79	25	21	0.9992	0.46
13	28	0.996	0.52				

lasting direct runoff.

A sensitivity analysis was performed for the catchment with the highest number of events (catchment ID: 12, n = 42). First, the effect of the 90 % threshold for direct runoff identification was examined. The parameter calibration procedure was run for a threshold value range (80–99 %) with 1 % increments. β_{opt}, BFI and all three calculated response time parameters were calculated and plotted (see Fig. 5). The relative change (compared to the 90 % value) in the calibrated β varies within the −0.001 – +0.002 interval, which does not cause a significant change in the resulting BFI values. However, the threshold strongly influences the resulting median T_c values, while T_L is barely influenced. It is also visible that using the same filter parameter with a higher threshold leads to higher times of concentration. This is expected since the increase in the threshold value leads to more prolonged direct runoff when the same filter parameter is used.

Second, the method's sensitivity on the choice of the r_{opt} value was assessed. The tested range of values was within 1–3 with a 0.1 increment. Fig. 6 presents the same results as for the threshold value (see above). It is clear that this choice has a stronger influence on the calibrated value of the filter parameter. β_{opt} shows stronger sensitivity to the value of r_{opt} in the range of 1–1.6, while the change in the value of β_{opt} becomes less significant with higher values of r_{opt}. However, BFI displays a constant decrease with the increase of r_{opt}. Time parameters (especially T_c) show an opposite behavior to β_{opt}. The sensitivity is higher with

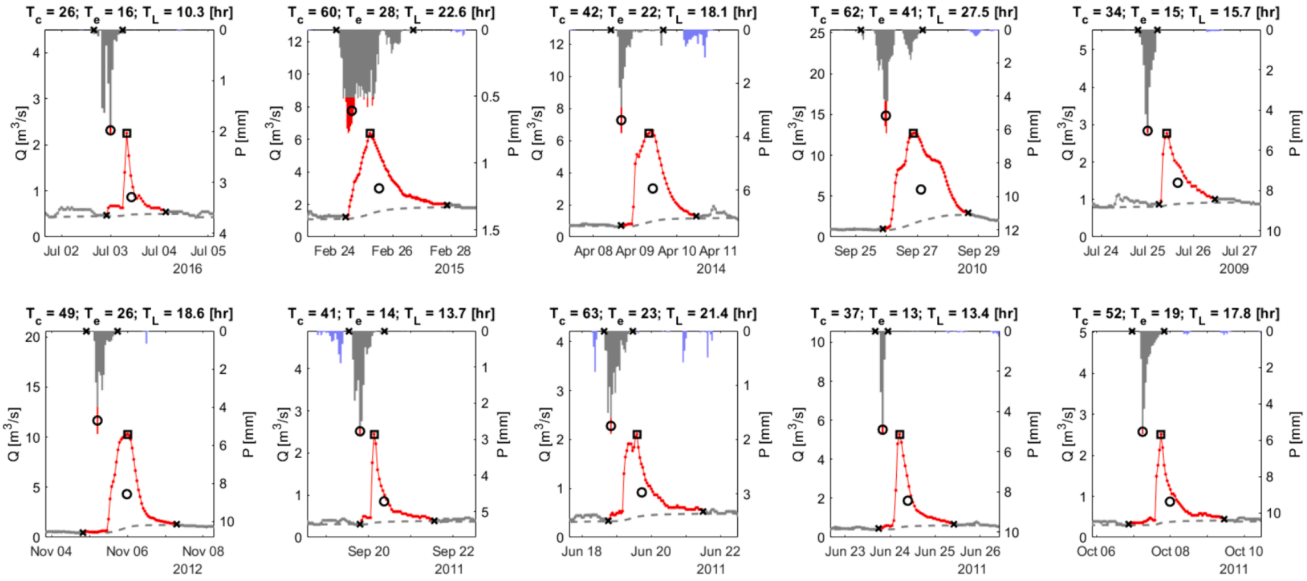

Fig. 3. Examples for the output plot of the proposed routine (catchment ID: 12). Red denotes excess precipitation and direct runoff, grey represents baseflow and infiltration loss, and the different markers show different time instants on the hydro- and hyetographs. (For interpretation of the references to colour in this figure legend, the reader is referred to the web version of this article.)

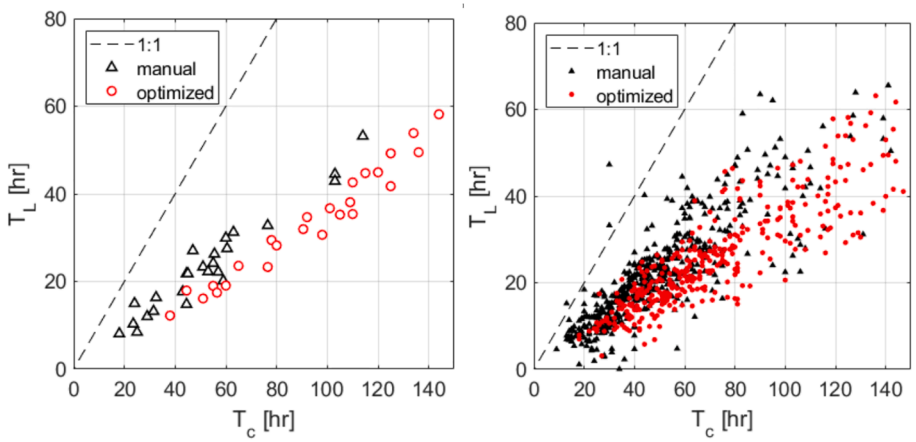

Fig. 4. Median (left) and event-based (right) catchment response times (T_L and T_c) obtained by manual calibration (manual) and the proposed method (optimized).

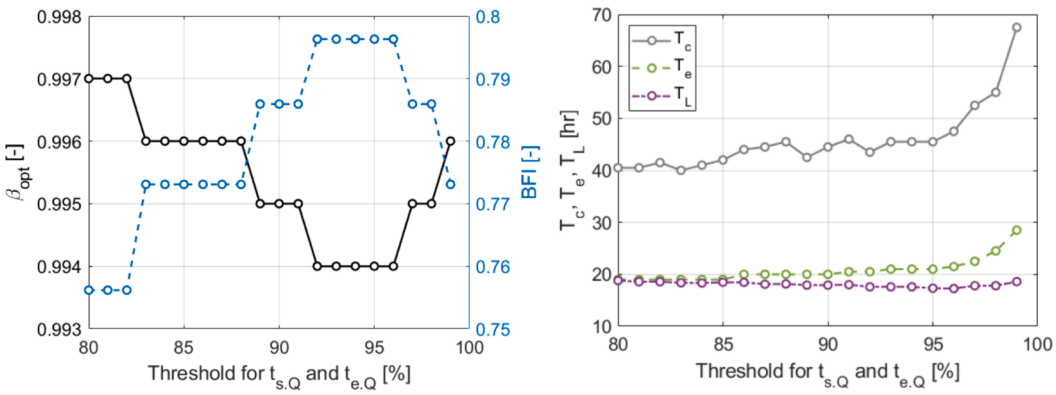

Fig. 5. Sensitivity of the proposed method to the value of the direct runoff selection threshold criteria. The calibrated parameter (β_{opt}) and the baseflow index (*BFI*) as a function of the threshold value (left). The median values of the time parameters (T_c, T_e, T_L) as a function of the threshold value (right).

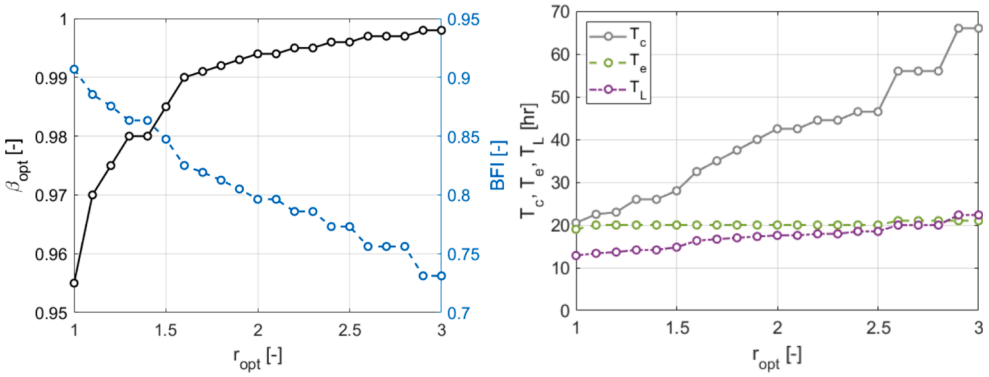

Fig. 6. Sensitivity of the proposed method to the value of the optimal ratio (r_{opt}) of T_c and T_e. The calibrated parameter (β_{opt}) and the baseflow index (*BFI*) as a function of r_{opt} (left). The median time parameters (T_c, T_e, T_L) as a function of r_{opt} (right).

higher β_{opt} (i.e., higher r_{opt}) values. Please note that in this case T_L shows a stronger sensitivity, not T_e, and T_L even grows longer than T_e in the case of high r_{opt} values.

Another significant aspect of the current method is the number of events used for calibration. To test the effect of event choice, events were selected randomly from the 42 available events. The whole range of 1 to 42 events was examined, testing 100 versions of event combinations in each case (when the number of possibilities allowed). This way, a set of β_{opt} values was created, hence, the median, 10th, and 90th percentiles could be determined. These values are plotted in Fig. 7. The median nearly always matches the value (β_{opt} = 0.995) using every event. However, as expected, the range of the β_{opt} values narrows as the number of events increases. The variability in the value of β_{opt} is more significant when 1–12 events are used, while it becomes zero over 34 events.

Another commonly mentioned T_c definition was also tested. T_c can also be defined as the time elapsed between the center of mass of effective precipitation and the end of direct runoff. The calibrated filter parameter (β_{opt} = 0.996) differed slightly from the one calibrated using the more often used definition (β_{opt} = 0.995). The resulting T_c values are presented in Fig. 8. Larger differences can be observed only for a few events but they do not significantly affect the median value. Note that even though the values should be larger for the new definition in case of the same filter parameter value, β_{opt} became slightly larger, hence, the changes can be observed in both directions across the 1:1 line.

Lastly, the baseflow index was calculated as a function of β and also as the number of passes (N). The latter determines the degree of smoothing (see the Introduction for more details). The implemented

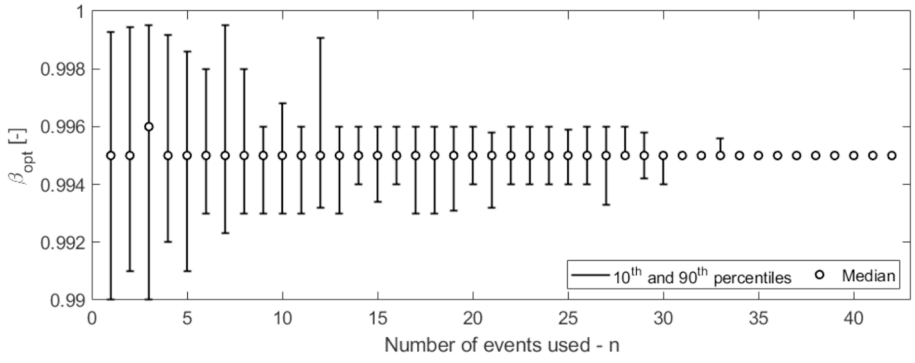

Fig. 7. The effect of the number of selected events (n) on the value of the calibrated parameter (β_{opt}).

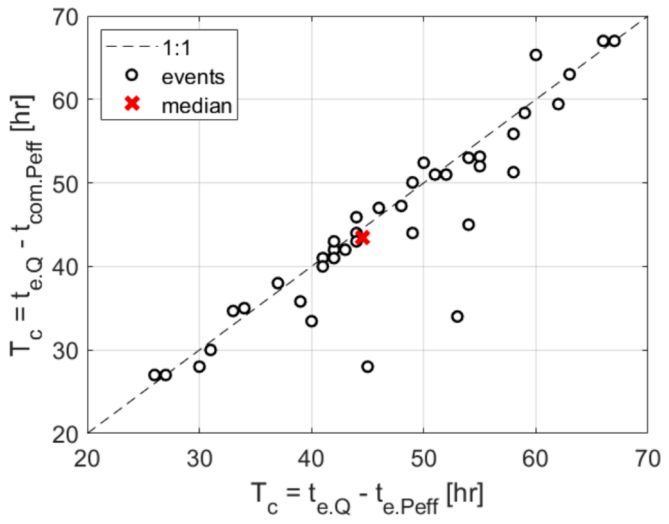

Fig. 8. Results of the different time of concentration definitions. The definition implemented in the proposed calibration routine is shown on the x-axis, and the other often-used definition is displayed on the y-axis.

case ($N = 3$) and the baseflow index resulting from the calibrated parameter value are plotted next to the general results in Fig. 9. The difference between the number of passes becomes negligible as β approaches unity. This is plausible since the higher the value of β, the flatter the baseflow time series, and additional passes cannot cause significant smoothing. The choice of β strongly impacts the resulting *BFI*, and the sensitivity is stronger at higher parameter values. The number of passes in itself has a less significant effect on *BFI*, namely −1.5 % – 2.5 %.

5. Discussion

The filter parameters and the corresponding baseflow indices obtained by the proposed calibration method appear to be somewhat higher than what is generally reported in other studies. Most studies, however, work with daily time series. Unfortunately, testing daily time resolution did not yield reliable results for the largest catchment since the smaller response time values are around one day. Nathan and McMahon (1990) originally tested three values for the filter parameter (0.9, 0.925, and 0.95) and found 0.925 generally acceptable for their study catchments. Several other authors (also working with daily observations) reported lower values than those presented in this study (Chapman, 1999; Mugo and Sharma, 1999; Szilagyi, 2004). However, the values calibrated by Szilagyi (2004) reached up to 0.999. Other studies using hourly or sub-hourly data reported generally higher values (Grimaldi et al., 2012; Tan et al., 2009). The effect of temporal resolution should be investigated in more detail, also related to the number of passes and in relation to the baseflow index. The baseflow indices obtained in this study correspond to the moderate/medium/high range of soil permeabilities, according to Bogena et al. (2005). Based on the Natural Resources Conservation Service dimensionless unit hydrograph procedure (Natural Resource Conservation Service, 1972, 1986), a linear relationship should exist between T_L and T_c. The fact that the linear correlation became more robust through the presented calibration process compared to manual calibration is a promising result. However, it does not guarantee that the presented values yield the 'true' baseflow. The relatively high calibrated filter parameter values can be understood through the findings of the sensitivity analysis.

The main results of the sensitivity analysis are that the i) proposed approach is not sensitive to the 90 % threshold criteria on the direct runoff's start and end times; ii) selection of r_{opt} has a stronger influence on β_{opt} when it is less than 1.6, but the effect on T_c is stronger when it is higher than 1.6; iii) number of applied events have a strong influence when it is smaller than a dozen, while the influence ceases when more than 30 events are employed; iv) two most often used T_c definitions yield similar results (especially for the median of event-based values), and; v) number of passes has the strongest influence near $\beta = 0.9$, however, this effect on the value of *BFI* is only a few percent.

The study catchments included in this paper do not cover a wide range in terms of some catchment properties, such as climate and soil characteristics. Hence, only one catchment was used to perform the sensitivity analysis. However, the proposed method could be tested for a continental or global set of catchments. If these would include catchment with larger areas, and thus longer response times, the effect of the temporal resolution could also be examined. Such a broad study would yield additional insight of the proposed approach.

6. Summary

The separation of stream flow into baseflow and direct runoff is an intricate task in hydrology. This paper provides a new methodology to calibrate the single parameter of the LH filter often used for baseflow separation. The proposed method combines a physically-based relationship of two different catchment response time definitions with their graphical interpretation. It is a step toward physically connecting the LH filter to the baseflow separation process. The results imply that the calibration routine yields acceptable results and can provide a general

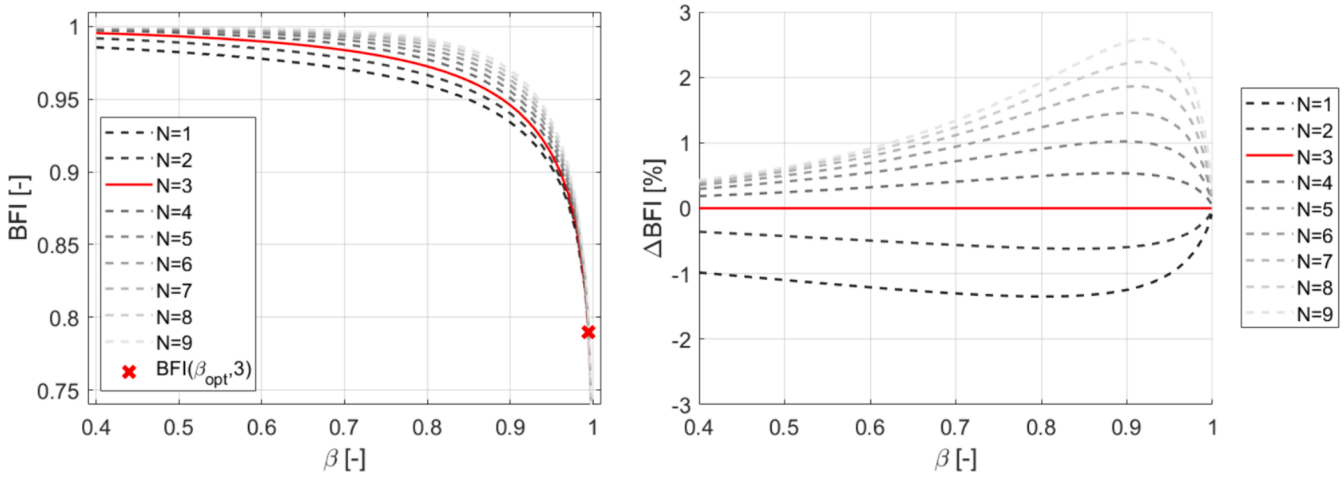

Fig. 9. The baseflow index (*BFI*) related to the value of the filter parameter (β) and the number of passes (N). Absolute value of *BFI* (left) and the relative change in the value of *BFI* (right).

framework for the LH filter's calibration. The routine is available in MATLAB and R, including sample data. Based on the presented results, the authors suggest using at least ten events per catchment while choosing single-peak events with a clear rising and falling limb.

The proposed routine could be investigated in more detail, especially regarding the time step of the observed precipitation and discharge time series. The performance of the presented method could be tested against baseflow derived from tracer measurements to get a deeper insight into its optimal applicability.

CRediT authorship contribution statement

Eszter D. Nagy: Conceptualization, Methodology, Software, Validation, Visualization, Writing – original draft. **Jozsef Szilagyi:** Writing – review & editing. **Peter Torma:** Writing – review & editing.

Declaration of competing interest

The authors declare that they have no known competing financial interests or personal relationships that could have appeared to influence the work reported in this paper.

Data availability

The authors do not have permission to share data.

Acknowledgements

The research presented in the article was carried out within the framework of the Széchenyi Plan Plus program with the support of the RRF 2.3.1 21 2022 00008 project. The first author was funded by the ÚNKP-22-4-I-BME-39 New National Excellence Program of the Ministry for Culture and Innovation from the source of the National Research, Development and Innovation Fund. The third author was supported by the Hungarian Academy of Sciences (Grant Nr. Janos Bolyai Fellowship 00906/23). Finally, the research was also supported by the Ministry of Culture and Innovation and the National Research, Development and Innovation Office (Grant Nr. TKP2021-NVA-02).

References

Almeida, I.K., Guarienti, J.A., Gabas, S.G., 2022. The time of concentration application in studies around the world: a review. Environ. Sci. Pollut. Res. 29 (6), 8126–8172. https://doi.org/10.1007/s11356-021-16790-2.

Babovic, V., Wu, Z. Y. (1994). Calibrating hydrodynamic models by means of simulated evolution. Proceedings of the First International Conference on Hydroinformatics (Hydroinformatics' 94), Rotterdam, Balkema.

Beven, K.J., 2020. A history of the concept of time of concentration. Hydrol. Earth Syst. Sci. 24, 2655–2670. https://doi.org/10.5194/hess-2019-588.

Bogena, H., Kunkel, R., Schöbel, T., Schrey, H.P., Wendland, F., 2005. Distributed modeling of groundwater recharge at the macroscale. *Ecol. Model.* 187 (1 SPEC. ISS), 15–26. https://doi.org/10.1016/j.ecolmodel.2005.01.023.

Boughton, W.C., 1988. Partitioning Streamflow by Computer. Transactions of the Institution of Engineers, Australia, Civil Engineering, pp. 285–291.

Chapman, T., 1999. A comparison of algorithms for stream flow recession and baseflow separation. Hydrol. Process. 13 (5), 701–714. https://doi.org/10.1080/02626668809491261.

Copernicus Climate Change Service (C3S) (2019). C3S ERA5-Land Reanalysis. Copernicus Climate Change Service, 2019.08.16.

Duncan, H.P., 2019. Baseflow separation - a practical approach. J. Hydrol. 575, 308–313. https://doi.org/10.1016/j.jhydrol.2019.05.040.

Eckhardt, K., 2005. How to construct recursive digital filters for baseflow separation. Hydrol. Process. 19 (2), 507–515. https://doi.org/10.1002/hyp.5675.

Eckhardt, K., 2008. A comparison of baseflow indices, which were calculated with seven different baseflow separation methods. J. Hydrol. 352 (1–2), 168–173. https://doi.org/10.1016/j.jhydrol.2008.01.005.

Furey, P.R., Gupta, V.K., 2001. A physically based filter for separating base flow from streamflow time series. Water Resour. Res. 37 (11), 2709–2722. https://doi.org/10.1029/2020WR028201.

Giani, G., Rico-Ramirez, M.A., Woods, R.A., 2021. A practical, objective, and robust technique to directly estimate catchment response time. Water Resour. Res. 57 (2), 1–17. https://doi.org/10.1029/2020WR028201.

Graszkiewicz, Z., Murphy, R.E., Hill, P.I., Nathan, R.J., 2011. Review of Techniques for Estimating the Contribution of Baseflow to Flood Hydrographs. In: In 33rd Hydrology and Water Resources Symposium, pp. 138–146.

Grimaldi, S., Petroselli, A., Tauro, F., Porfiri, M., 2012. Time of concentration: a paradox in modern hydrology. Hydrol. Sci. J. 57 (2), 217–228. https://doi.org/10.1080/02626667.2011.644244.

Jolánkai, Z.s., Koncsos, L., 2018. Base flow index estimation on gauged and ungauged catchments in hungary using digital filter, multiple linear regression and artificial neural networks. Periodica Polytechnica Civil Engineering 62 (2), 363–372. https://doi.org/10.7158/W12-028.2013.17.1.

Ladson, A.R., Brown, R., Neal, B., Nathan, R., 2013. A standard approach to baseflow separation using the lyne and hollick filter. Aust. J. Water Resour. 17 (1), 25–34. https://doi.org/10.7158/W12-028.2013.17.1.

Langridge, M., Gharabaghi, B., McBean, E., Bonakdari, H., Walton, R., 2020. Understanding the dynamic nature of time-to-peak in UK streams. J. Hydrol. 583, 124630 https://doi.org/10.1016/j.jhydrol.2020.124630.

Li, L., Maier, H.R., Partington, D., Lambert, M.F., Simmons, C.T., 2014. Performance assessment and improvement of recursive digital baseflow filters for catchments with different physical characteristics and hydrological inputs. Environ. Model. Softw. 54, 39–52. https://doi.org/10.1016/j.envsoft.2013.12.011.

Linsley, R.K., Kohler, M.A., Paulhus, J.L.H., Wallace, J.S., 1958. Hydrology for Engineers. McGraw & Hill, New York.

Lott, D.A., Stewart, M.T., 2013. A power function method for estimating base flow. Ground Water 51 (3), 442–451. https://doi.org/10.1111/j.1745-6584.2012.00980.x.

Lyne, V., Hollick, M., 1979. Stochastic Time-Variable Rainfall-Runoff Modeling. Hydrology and Water Resources Symposium. Institution of Engineers, Australia, Perth, pp. 89–92.

Madsen, H., Wilson, G., Ammentorp, H.C., 2002. Comparison of different automated strategies for calibration of rainfall-runoff models. J. Hydrol. 261 (1–4), 48–59. https://doi.org/10.1016/S0022-1694(01)00619-9.

Mei, Y., Anagnostou, E.N., 2015. A hydrograph separation method based on information from rainfall and runoff records. J. Hydrol. 523, 636–649. https://doi.org/10.1016/j.jhydrol.2015.01.083.

Meshgi, A., Schmitter, P., Babovic, V., Chui, T.F.M., 2014. An empirical method for approximating stream baseflow time series using groundwater table fluctuations. J. Hydrol. 519 (A), 1031–1041. https://doi.org/10.1016/j.jhydrol.2014.08.033.

Meshgi, A., Schmitter, P., Chui, T.F.M., Babovic, V., 2015. Development of a modular streamflow model to quantify runoff contributions from different land uses in tropical urban environments using Genetic Programming. J. Hydrol. 525, 711–723. https://doi.org/10.1016/j.jhydrol.2015.04.032.

Mugo, J.M., Sharma, T.C., 1999. Application of a Conceptual Method for Separating Runoff Components in Daily Hydrographs in Kimakia Forest Catchments, Kenya. *Hydrological Processes* 13 (17), 2931–2939. https://doi.org/10.1002/(SICI)1099-1085(19991215)13:17<2931::AID-HYP838>3.0.CO;2-N.

Nagy, E.D., Szilagyi, J., Torma, P., 2021. Assessment of dimension-reduction and grouping methods for catchment response time estimation in hungary. Journal of Hydrology: Regional Studies 38, 100971. https://doi.org/10.1016/j.ejrh.2021.100971.

Nagy, E.D., Szilagyi, J., Torma, P., 2022. Estimation of catchment response time using a new automated event-based approach. J. Hydrol. 613, 128355 https://doi.org/10.1016/j.jhydrol.2022.128355.

Nathan, R.J., McMahon, T.A., 1990. Evaluation of automated techniques for base flow and recession analyses. Water Resour. Res. 26 (7), 1465–1473. https://doi.org/10.1029/WR026i007p01465.

Natural Resource Conservation Service (1972). *Hydrology*. National engineering handbook, Sec. 4, U.S. Department of Agriculture, Washington, D.C.

Natural Resource Conservation Service (1986). *Urban hydrology for small watersheds*. Technical Release 55, Washington, D.C.

Nejadhashemi, A.P., Shirmohammadi, A., Montas, H.J., Sheridan, J.M., Bosch, D.D., 2007. Analysis of watershed physical and hydrological effects on baseflow separation. J. Hydrol. Eng. 13 (10), 971–980. https://doi.org/10.1061/(ASCE)1084-0699(2008)13:10(971).

Nejadhashemi, A.P., Shirmohammadi, A., Sheridan, J.M., Montas, H.J., Mankin, K.R., 2009. Case study: evaluation of streamflow partitioning methods. J. Irrig. Drain. Eng. 135 (6), 791–801. https://doi.org/10.1061/(ASCE)IR.1943-4774.0000093.

Partington, D., Brunner, P., Simmons, C.T., Werner, A.D., Therrien, R., Maier, H.R., Dandy, G.C., 2012. Evaluation of outputs from automated baseflow separation methods against simulated baseflow from a physically based, surface water-groundwater flow model. J. Hydrol. 458–459, 28–39. https://doi.org/10.1016/j.jhydrol.2012.06.029.

Schwartz, S.S., 2007. Automated algorithms for heuristic base-flow separation. J. Am. Water Resour. Assoc. 43 (6), 1583–1594.

Stadnyk, T.A., Gibson, J.J., Longstaffe, F.J., 2015. Basin-scale assessment of operational base flow separation methods. J. Hydrol. Eng. 20 (5) https://doi.org/10.1061/(ASCE)HE.1943-5584.0001089.

Stewart, M., Cimino, J., Ross, M., 2007. Calibration of base flow separation methods with streamflow conductivity. Ground Water 45 (1), 17–27. https://doi.org/10.1111/j.1745-6584.2006.00263.x.

Szilagyi, J., 2004. Heuristic continuous base flow separation. J. Hydrol. Eng. 9 (4), 311–318. https://doi.org/10.1061/(asce)1084-0699(2004)9:4(311).

Tan, S.B., Lo, E.-Y.-M., Shuy, E.B., Chua, L.H., Lim, W.H., 2009. Hydrograph separation and development of empirical relationships using single-parameter digital filters. J. Hydrol. Eng. 14 (3), 271–279. https://doi.org/10.1061/(asce)1084-0699(2009)14:3(271).

Tang, W., Carey, S.K., 2017. HydRun: A MATLAB toolbox for rainfall-runoff analysis. Hydrol. Process. 31 (15), 2670–2682. https://doi.org/10.1002/hyp.11185.
Wong, T.S.W., 2003. Comparison of celerity-based with velocity-based time-of-concentration of overland plane and time-of-travel in channel with upstream inflow. Adv. Water Resour. 26 (11), 1171–1175. https://doi.org/10.1016/S0309-1708(03)00108-8.
Xie, J., Liu, X., Wang, K., Yang, T., Liang, K., Liu, C., 2020. Evaluation of typical methods for baseflow separation in the contiguous United States. J. Hydrol. 583, 124628 https://doi.org/10.1016/j.jhydrol.2020.124628.
Zhang, J., Zhang, Y., Song, J., Cheng, L., 2017. Evaluating relative merits of four baseflow separation methods in eastern Australia. J. Hydrol. 549, 252–263. https://doi.org/10.1016/j.jhydrol.2017.04.004.
Zheng, M., 2015. Estimation of Base Flow Using Flow-Sediment Relationships in the Chinese Loess Plateau. Catena 125, 129–134. https://doi.org/10.1016/j.catena.2014.10.020.